POTENTIAL OF AUTOMATED DIGITAL HEMISPHERICAL PHOTOGRAPHY AND WIRELESS QUANTUM SENSORS FOR ROUTINE CANOPY MONITORING AND SATELLITE PRODUCT VALIDATION

Luke A. Brown[1], Harry Morris[1], Erika Albero[2], Ernesto Lopez-Baeza[2], Frank Tiedemann[3], Lukas Siebicke[3], Alexander Knohl[3], Carolina da Silva Gomes[4], Gabriele Bai[4], Christophe Lerebourg[4], Nadine Gobron[5], Christian Lanconelli[5], Marco Clerici[5], Darius Culvenor[6] and Jadunandan Dash[1]*

[1]School of Geography and Environmental Science, University of Southampton, *l.a.brown@soton.ac.uk
[2]Department of Earth Physics and Thermodynamics, University of Valencia, [3]Bioclimatology, University of Göttingen, [4]ACRI-ST, [5]European Commission Joint Research Centre, [6]Environmental Sensing Systems

ABSTRACT

To better characterize the temporal dynamics of vegetation biophysical variables, a variety of automated *in* situ measurement techniques have been developed in recent years. In this study, we investigated automated digital hemispherical photography (DHP) and wireless quantum sensors, which were installed at two sites under the Copernicus Ground Based Observations for Validation (GBOV) project. Daily estimates of plant area index (PAI) and the fraction of absorbed photosynthetically active radiation (FAPAR) were obtained, which realistically described expected vegetation dynamics. Good correspondence with manual DHP and LAI-2000 data (RMSE = 0.39 to 0.90 for PAI, RMSE = 0.07 for FAPAR) provided confidence that the investigated approaches can deliver data of comparable quality to traditional *in situ* measurement techniques.

Index Terms— DHP, FAPAR, GBOV, LAI, PAI

1. INTRODUCTION

In situ measurements of vegetation biophysical variables are needed in agricultural and forest monitoring, and for the validation of satellite products, which are used in a range of downstream applications. Because periodic field campaigns are unable to provide detailed information on vegetation temporal dynamics, in recent years, a variety of automated measurement techniques have been developed [1]–[5]. In this study, we investigate automated digital hemispherical photography (DHP) and wireless quantum sensors installed under the Copernicus Ground Based Observations for Validation (GBOV) project (https://land.copernicus.eu/global/gbov). Their potential for monitoring plant area index (PAI) and the fraction of absorbed photosynthetically active radiation (FAPAR) is assessed, as is their utility for decametric satellite product validation.

2. MATERIALS AND METHODS

2.1. Automated DHP

An automated DHP system was deployed at Hainich National Park, Germany (51.0794°N, 10.4532°E), in August 2019 (Figure 1). The site is characterized by old-growth beech forest. The automated DHP system consisted of two modified Harbortronics Cyclapse time-lapse digital cameras, each comprising a waterproof housing with acrylic dome, a DigiSnap Pro intervalometer, and a Canon EOS 1300D digital single-lens reflex (DLSR) camera equipped with a Sigma 4.5mm F2.8 EX DC fisheye lens. Power was provided through a mains supply available at the site, and using a cellular modem, acquired images were automatically transferred to a remote server via file transfer protocol (FTP). The set of two cameras was mounted on a steel pole 1.3 m above the ground, in the centre of a plot routinely sampled under the Integrated Carbon Observation System (ICOS) programme. To capture both the understory and overstory, one camera was oriented directly upwards, whilst the second was oriented directly downwards (Figure 1).

Figure 1: Automated DHP system deployed at Hainich National Park, Germany (left) and example upwards- (top right) and downwards- (bottom right) facing images.

Following the approach of [6], each camera was configured to collect raw images every 30 minutes between 05:00 and 21:00 local time, ensuring images close to sunrise and sunset were captured. To derive plant area (PAI), raw images were classified as the vegetation canopy or its background. The classification algorithms of [7] and [8] were adopted for upwards- and downwards-facing images, respectively. Once classified, each image was split into zenith and azimuth bins of 10°. PAI was calculated as

$$PAI = 2\sum_{i=1}^{n} -\overline{\ln P(\theta_i)} \cos\theta_i \sin\theta_i \, \mathrm{d}\,\theta_i \quad (1)$$

where $\overline{\ln P(\theta_i)}$ is the mean of the natural logarithm of gap fraction values over all azimuth bins at zenith angle θ_i (± 5°) [9]. By taking the mean of the natural logarithm of gap fraction values, the effects of foliage clumping were accounted for according to [10].

To suppress spurious values and noise caused by variations in illumination conditions, data screening of the resulting PAI time-series was needed. In a previous study [6], data were successfully screened by selecting the maximum value in each day. In this study, we adopted an alternative data screening approach. For upwards-facing images, the PAI value closest to sunset was selected [11], whereas for downwards-facing images, the mean PAI between 11:00 and 13:00 local time was calculated to suppress shadows [12].

2.2. Wireless quantum sensors

A wireless quantum sensor network was deployed at the Valencia Anchor Station, Spain (39.5708N, 1.2882E), in March 2020 (Figure 2). The site is characterized by Mediterranean vineyard vegetation. The sensor network consisted of 12 nodes, each comprising an Environmental Sensing Systems solar-powered data logger and four Apogee Instruments SQ-110 quantum sensors. Each data logger was equipped with a wireless radio, enabling transmission of data to a base station. The base station aggregates the data received from each node, and using a cellular modem, automatically uploads these data to a remote server.

Figure 2: Wireless quantum sensor network deployed at the Valencia Anchor Station, Spain.

The 12 nodes were distributed over a 60 m x 60 m plot, with an even number of nodes located within and between rows to reflect the mixture of vegetation and bare soil experienced at the site (Figure 2). At each node, a pair of sensors was positioned above and below the canopy, enabling the measurement of incoming and outgoing terms. Each node was configured to collect PAR data every 5 minutes. Using these data, we determined 4-flux instantaneous FAPAR as

$$FAPAR_{4-flux} = \frac{I_{TOC}^{\downarrow} - I_{ground}^{\downarrow} + I_{ground}^{\uparrow} - I_{TOC}^{\uparrow}}{I_{TOC}^{\downarrow}} \quad (2)$$

where $I_{TOC}^{\downarrow}$, $I_{TOC}^{\uparrow}$, $I_{ground}^{\downarrow}$, and $I_{ground}^{\uparrow}$ represent the mean incoming and outgoing PAR values recorded by all nodes at the top of canopy and ground at 10:00 local solar time (± 15 minutes). We also calculated a 2-flux estimate as

$$FAPAR_{2-flux} = 1 - \frac{I_{ground}^{\downarrow}}{I_{TOC}^{\downarrow}} \quad (3)$$

2.3. Manual sampling

To verify the estimates of PAI and FAPAR provided by the automated DHP system and wireless quantum sensor network at the two sites, additional field data collection was carried out throughout the growing season. This involved manual sampling at 13 (21) locations within the 40 m x 40 m (60 m x 60 m) plot containing the automated DHP system (wireless quantum sensor network). DHP data were processed as described in Section 2.1 to estimate PAI. FAPAR was approximated as the instantaneous black-sky fraction of intercepted photosynthetically active radiation (FIPAR), which was calculated as

$$FIPAR = 1 - \overline{P(\theta_{SZA})} \quad (4)$$

where $\overline{P(\theta_{SZA})}$ is the mean gap fraction over all images and azimuth bins at the solar zenith angle at 10:00 local solar time (± 5°) [13], [14]. Additionally, at Hainich National Park, LI-COR LAI-2000 data were also acquired and processed.

3. PRELIMINARY RESULTS

3.1. PAI at Hainich National Park

The data screening approach described in Section 2.1 appeared successful in suppressing the majority of noise in the PAI data, providing time-series that reflected expected vegetation dynamics, realistically capturing the end of the 2019 growing season, the senescent period, and the start and peak of the 2020 growing season (Figure 3). The understory layer was found to have a considerable contribution to the total PAI, particularly during the early spring, highlighting the importance of characterizing both the understory and overstory when collecting *in situ* data. Overstory PAI values

appeared slightly lower in the summer of 2019 than 2020. An explanation is that during installation, the camera was set to default exposure metering, whereas in October 2019, it was adjusted to 'centre-weighted average' metering, which is more appropriate for circular fisheye images. For both layers, the automated DHP data demonstrated good agreement with the manual DHP data acquired at 13 sampling locations in the surrounding 40 m x 40 m plot (RMSE = 0.61 to 0.90). For the overstory, good agreement with LAI-2000 data was also observed (RMSE = 0.39).

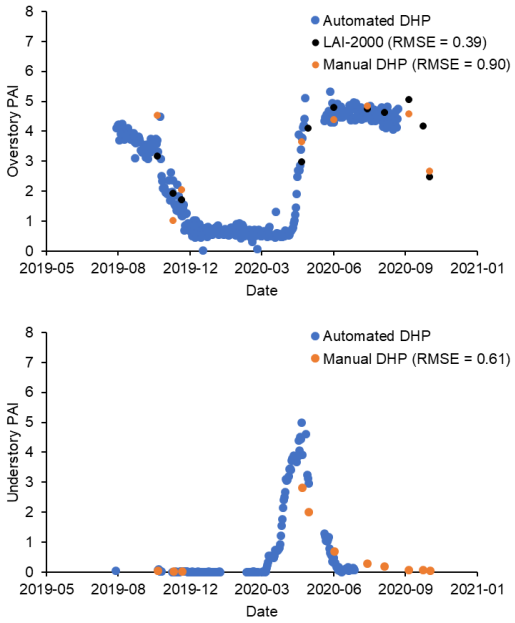

Figure 3: Time-series of PAI derived from the upwards (top) and downwards (bottom) facing automated DHP systems at Hainich National Park, in addition to estimates of PAI derived from manually acquired DHP and LAI-2000 data over the surrounding 40 m x 40 m plot on several dates.

3.2. FAPAR at the Valencia Anchor Station

The wireless quantum sensor network was able to realistically capture expected vegetation dynamics at the Valencia Anchor Station, including the senescent period, start, and peak of 2020 growing season (Figure 4). Despite the bright soil background experienced at the site, very little difference between the 4-flux and 2-flux estimates of FAPAR was observed. As similar results were recently obtained by [15], this is a useful finding for planning future validation activities, given the extra cost and effort associated with 4-flux measurements. Again, good correspondence was achieved with the manual DHP data collected over the 60 m x 60 m plot containing the sensor network (RMSE = 0.07).

4. DISCUSSION AND CONCLUSION

4.1. Utility of automated instrumentation

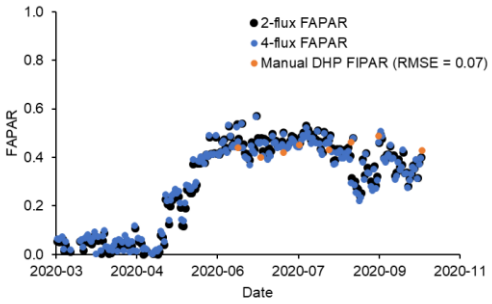

Figure 4: Time-series of 2-flux and 4-flux FAPAR derived from the wireless quantum sensor network at the Valencia Anchor Station, in addition to estimates of FIPAR derived from manually acquired DHP images over the 60 m x 60 m plot on several dates.

The preliminary results presented in this study highlight the potential of automated, permanently deployed instrumentation to provide rich temporal characterization of vegetation dynamics over spatial extents useful for decametric satellite product validation. The daily time-series offered by such systems mean that contemporaneous *in situ* data are available whenever cloud-free satellite images are acquired over equipped study sites. The fact that the PAI and FAPAR values derived from our automated DHP system and wireless quantum sensor network achieved good correspondence with manual DHP and LAI-2000 data provides confidence in their ability to deliver data of comparable quality to traditional *in situ* measurement approaches at the plot scale.

When compared to periodic field campaigns, automated, permanently deployed instrumentation will enable considerable progress to Stage 3 of the Committee on Earth Observation Satellites (CEOS) Working Group on Calibration and Validation (WGCV) Land Product Validation (LPV) hierarchy, in which 'uncertainties are characterized in a statistically robust way over multiple locations and time periods representing global conditions' [16]. Having said this, since permanently deployed instruments can only cover a limited number of locations, it is clear that periodic field campaigns will continue to play an important role, enabling biases (e.g. due to inadequate spatial representativeness) to be identified and corrected for.

4.2. Future work

Although our preliminary results demonstrate the potential of automated DHP and wireless quantum sensors for continuous vegetation monitoring and satellite product validation, there is considerable opportunity for future work. For example, whilst a time-series of PAI was derived from the automated DHP system, a key advantage of the approach is the ability to derive other biophysical variables including FIPAR and the fraction of vegetation cover (FCOVER) [13], [14]. Similarly, approaches to estimate PAI from wireless quantum sensors (e.g. using data collected at a solar zenith angle of 57.5°, or

by making use of ancillary data on canopy leaf angle distribution) are also available [3], [5], and should be explored. Further evaluation of the automated DHP processing methods could also be envisaged (e.g. through comparison with a subset of manually classified images). Additionally, differences in the definition of *in situ* and satellite-derived quantities (e.g. PAI vs. LAI, green FAPAR vs. total FAPAR) should be considered.

Though already useful for validating decametric satellite products such as those from Sentinel-2, to make the temporally continuous *in situ* data provided by the systems described in this study useful for validating moderate spatial resolution satellite products, appropriate upscaling approaches are required. Recent progress using multi-temporal transfer functions and radiative transfer model-based approaches has been made [17]–[19], and future work will evaluate these methods over our study sites.

In addition to maximizing the utility of the data already being collected, there is also a need to expand the geographical coverage of such installations. Several new sites will be equipped with automated DHP systems and wireless quantum sensor networks in 2021, with a particular focus on under-characterized regions. These include tropical woody savanna (Litchfied, Australia) and temperate Eucalypt forest (Wombat, Australia) sites.

5. ACKNOWLEDGEMENT

This study has been undertaken using data from GBOV 'Ground Based Observations for Validation' (https://land.copernicus.eu/global/gbov) funded by the European Commission Joint Research Centre FWC 932059, part of the Global Component of the European Union's Copernicus Land Monitoring Service.

6. REFERENCES

[1] Y. Ryu *et al.*, "Continuous observation of tree leaf area index at ecosystem scale using upward-pointing digital cameras," *Remote Sens. Environ.*, vol. 126, pp. 116–125, Nov. 2012.

[2] D. Culvenor, G. Newnham, A. Mellor, N. Sims, and A. Haywood, "Automated In-Situ Laser Scanner for Monitoring Forest Leaf Area Index," *Sensors*, vol. 14, no. 8, pp. 14994–15008, Aug. 2014.

[3] Y. Qu *et al.*, "LAINet – A wireless sensor network for coniferous forest leaf area index measurement: Design, algorithm and validation," *Comput. Electron. Agric.*, vol. 108, pp. 200–208, Oct. 2014.

[4] B. Brede *et al.*, "Monitoring Forest Phenology and Leaf Area Index with the Autonomous, Low-Cost Transmittance Sensor PASTiS-57," *Remote Sens.*, vol. 10, no. 7, p. 1032, Jun. 2018.

[5] M. Toda and A. D. Richardson, "Estimation of plant area index and phenological transition dates from digital repeat photography and radiometric approaches in a hardwood forest in the Northeastern United States," *Agric. For. Meteorol.*, no. September, pp. 1–10, Sep. 2017.

[6] L. A. Brown, B. O. Ogutu, and J. Dash, "Tracking forest biophysical properties with automated digital repeat photography: A fisheye perspective using digital hemispherical photography from below the canopy," *Agric. For. Meteorol.*, vol. 287, p. 107944, Jun. 2020.

[7] T. W. Ridler and S. Calvard, "Picture Thresholding Using an Iterative Selection Method," *IEEE Trans. Syst. Man. Cybern.*, vol. 8, no. 8, pp. 630–632, 1978.

[8] G. E. Meyer and J. C. Neto, "Verification of color vegetation indices for automated crop imaging applications," *Comput. Electron. Agric.*, vol. 63, no. 2, pp. 282–293, Oct. 2008.

[9] J. Miller, "A formula for average foliage density," *Aust. J. Bot.*, vol. 15, no. 1, pp. 141–144, Apr. 1967.

[10] A. R. G. Lang and X. Yueqin, "Estimation of leaf area index from transmission of direct sunlight in discontinuous canopies," *Agric. For. Meteorol.*, vol. 37, no. 3, pp. 229–243, Aug. 1986.

[11] N. J. J. Bréda, "Ground-based measurements of leaf area index: a review of methods, instruments and current controversies," *J. Exp. Bot.*, vol. 54, no. 392, pp. 2403–2417, Sep. 2003.

[12] A. D. Richardson, B. H. Braswell, D. Y. Hollinger, J. P. Jenkins, and S. V. Ollinger, "Near-surface remote sensing of spatial and temporal variation in canopy phenology," *Ecol. Appl.*, vol. 19, no. 6, pp. 1417–1428, Sep. 2009.

[13] M. Weiss *et al.*, "On Line Validation Exercise (OLIVE): A Web Based Service for the Validation of Medium Resolution Land Products. Application to FAPAR Products," *Remote Sens.*, vol. 6, no. 5, pp. 4190–4216, May 2014.

[14] W. Li *et al.*, "A Generic Algorithm to Estimate LAI, FAPAR and FCOVER Variables from SPOT4_HRVIR and Landsat Sensors: Evaluation of the Consistency and Comparison with Ground Measurements," *Remote Sens.*, vol. 7, no. 12, pp. 15494–15516, Nov. 2015.

[15] W. Li, H. Fang, S. Wei, M. Weiss, and F. Baret, "Critical analysis of methods to estimate the fraction of absorbed or intercepted photosynthetically active radiation from ground measurements: Application to rice crops," *Agric. For. Meteorol.*, vol. 297, no. December 2020, p. 108273, Feb. 2021.

[16] R. Fernandes *et al.*, "Global Leaf Area Index Product Validation Good Practices," in *Best Practice for Satellite-Derived Land Product Validation*, 2.0., R. Fernandes, S. Plummer, and J. Nightingale, Eds. Land Product Validation Subgroup (Committee on Earth Observation Satellites Working Group on Calibration and Validation), 2014.

[17] G. Yin *et al.*, "Derivation of temporally continuous LAI reference maps through combining the LAINet observation system with CACAO," *Agric. For. Meteorol.*, vol. 233, pp. 209–221, Feb. 2017.

[18] M. Campos-Taberner *et al.*, "Multitemporal Monitoring of Plant Area Index in the Valencia Rice District with PocketLAI," *Remote Sens.*, vol. 8, no. 3, p. 202, Mar. 2016.

[19] L. A. Brown, B. Ogutu, F. Camacho, B. Fuster, and J. Dash, "Deriving Leaf Area Index Reference Maps Using Temporally Continuous In Situ Data: A Comparison of Upscaling Approaches," *IEEE J. Sel. Top. Appl. Earth Obs. Remote Sens.*, vol. 14, 2021.